Comparative study of fault-tolerant performance of a segmented rotor SRM and a conventional SRM

X. SUN[1,2]*, Z. XUE[1], S. HAN[3], L. CHEN[2], X. XU[2], and Z. YANG[3]

[1]School of Automotive and Traffic Engineering, Jiangsu University, Zhenjiang 212013, China
[2]Automotive Engineering Research Institute, Jiangsu University, Zhenjiang 212013, China
[3]School of Electrical and Information Engineering, Jiangsu University, Zhenjiang 212013, China

Abstract. Due to the separation of magnetic field, electrical isolation and thermal isolation, motor drives possess a high fault-tolerance characteristic. In this paper, comparative study of mutual inductance between the proposed segmented rotor switched reluctance motor (SSRM) and the conventional switched reluctance motor (SRM) is carried out first, illustrating that the proposed SSRM has less mutual inductance between phases than the conventional SRM. In addition, if winding faults or power converter faults lead to phase failure, a comparative analysis on fault-tolerant performance under phase failure condition between the proposed SSRM and the conventional SRM is simulated in detail using the finite element method (FEM). Simulation results reveal that dynamic performance of the proposed SSRM, including output torque and phase current, is better than that of the conventional SRM. That is, the capacity of operating with the fault under phase failure condition in the proposed SSRM is superior to that in the conventional SRM.

Key words: fault tolerance, segmented rotor SRM, phase failure, finite element method, dynamic performance.

1. Introduction

In recent years, demands of energy conservation and emission reduction have put pressure on automotive industry to develop hybrid electric vehicles [1–3]. The belt-driven starter/generator (BSG) is gaining more and more attention in hybrid vehicles in which high reliability must be ensured, because any kinds of faults would cause serious effects on continual operation [4–7]. Therefore, more attention focused on the demand for fault-tolerant motors.

Induction motor (IM) and permanent-magnet motor (PM) are the prime alternatives to the BSG. Unfortunately, acquiring high torque at low speed for IM is difficult; for PM, its high cost, due to the permanent magnet and demagnetization under high temperatures, has degraded its performance and limited its promotion [4, 5, 7–11]. Though new structures and new materials of PMs have improved their performance [12–15], nevertheless, the fault-tolerant performances of IM and PM are rarely reported and are less than satisfactory [16–18].

A conventional switched reluctance motor (SRM) is a doubly-salient and single-excited motor where the windings are wound in stator poles and there are no windings or permanents in the rotor. These structures lead to many distinguished merits, such as robustness, low cost, and wide applications in serious environment and high speeds [19]. Therefore, applying the SRM to the BSG can not only satisfy the requirements of fault tolerance but could also be an academic novelty. However, the fault-tolerant capability of the conventional SRM is limited, a novel segmented rotor SRM (SSRM) is proposed in this paper to improve the fault-tolerant performance in structure design instead of power converter or control.

In order to highlight the advantages of the proposed SSRM, comparative analysis on dynamic performance between the proposed SSRM and the conventional SRM by means of finite element method (FEM) is developed in throughout the paper. In the following, the concept and topology of the SSRM and SRM are briefly introduced in Section 2. Then in Section 3, mutual inductance between the proposed SSRM and the conventional SRM is evaluated based on FEM. Thereafter, comparative analysis on fault-tolerant performance under phase failure condition between the proposed SSRM and the conventional SRM is presented in detail in Section 4, followed by the conclusions in Section 5.

2. Concept and topology

The cross-sectional views of the proposed SSRM and the conventional SRM are shown in Fig. 1. In the four-phase
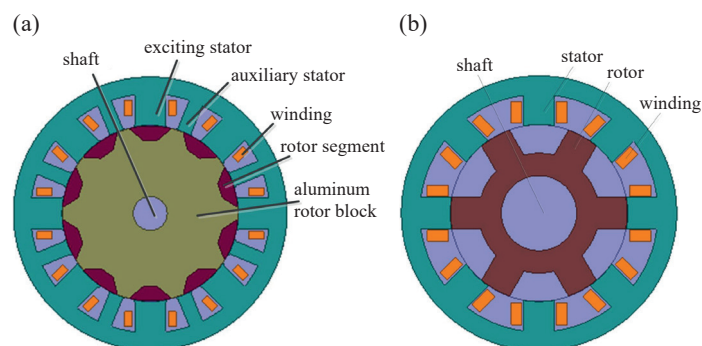

Fig. 1. Cross-sectional views of the proposed 16/10 SSRM and the conventional 8/6 SRM: a) proposed 16/10 SSRM, b) conventional 8/6 SRM

16/10-pole SSRM (Fig. 1a) the stator has two types of poles – exciting and auxiliary poles. The exciting stator poles are wound by concentrated windings, which are short and non-overlap the end-windings, while the auxiliary stator poles are not wound by any windings, only providing the flux return path. In addition, it can be seen that the rotor is composed of a series of discrete segments, and that each segment is embedded in an aluminum rotor block without any mechanical saliency and is magnetically isolated from its neighbors, which may improve the fault-tolerant capacity. The materials of the lamination and shaft are DW310–35 and steel, respectively. Table 1 shows the specifications of the proposed SSRM and the conventional SRM.

Table 1
Specifications of the SRMs

parameters	SSRM	SRM
number of phases	4	4
outer radius of stator (mm)	64	64
outer radius of rotor (mm)	41	41
length of stack (mm)	80	80
length of airgap (mm)	0.25	0.25
stator yoke thickness (mm)	8	8.7
stator pole arc (°)	21.375/10.69	20.25
rotor pole arc (°)	26.64	21
number of turns	26	34
wire diameter (mm)	2	2.24
slot factor	0.82	0.56
resistance per phase (mΩ)	18.5	28.1

3. Comparisons of mutual inductance

Owing to the separation of magnetic field, electrical isolation, and thermal isolation, the SSRM drive possesses a high fault-tolerance characteristic. Thanks to the auxiliary stator poles, the fluxes generated by one exciting stator pole are hard to couple with other stator poles, which guarantees the separation of magnetic field. The asymmetric half-bridge converter, which will be introduced in section 4.1, is used for each phase in order to decouple phases electrically. Furthermore, phase-phase fault is reduced because the end-windings do not overlap, which ensures electrical isolation. As described in section 2, the different phase windings are physically separated by the unwound stator teeth and therefore, if one phase is under fault and the temperature rises, the thermal transfer between windings can be stopped by the stator core, which ensures proper temperature in healthy windings and enables them to operate normally. In this paper, the high fault-tolerance can be evaluated by the independence between adjacent phases. The independence between adjacent phases can be described by the ratio of the mutual inductance to the self-inductance [20].

To enhance the starting capability and load capacity at low speed of the SRMs, two-phase excitation and chopped current control (CCC) are usually adopted [21]. Thus, the magnetic field at this excitation will differ from that at one-phase exci-

tation and mutual inductance will change significantly. In this paper, the difference of flux linkage between two-phase excitation and one-phase excitation is employed to quantitatively describe the mutual inductance.

Taking phase A and phase B as the research objects, the flux linkages of the phase windings versus the phase current when phase A is at the aligned position in the conventional SRM and the proposed SSRM are shown in Figs. 2 and 3.
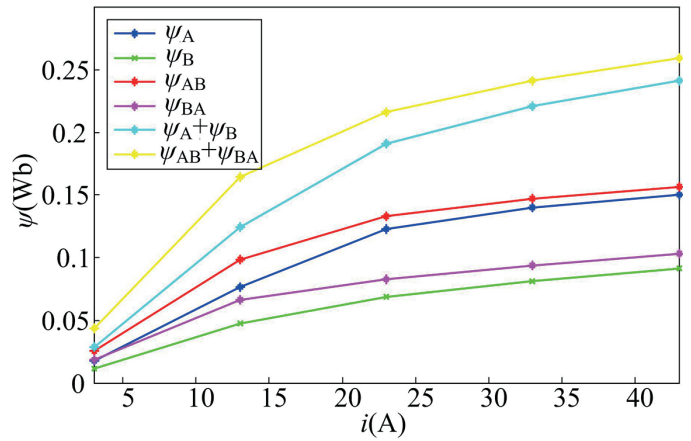

Fig. 2. Flux linkage versus the phase current when phase A is at the aligned position in the conventional SRM
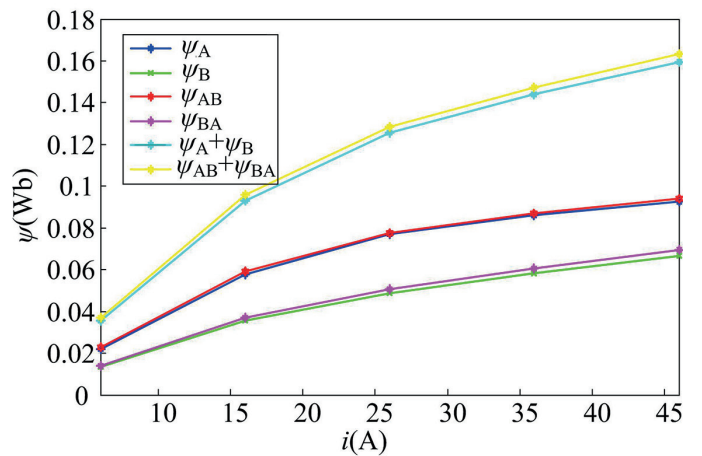

Fig. 3. Flux linkage versus the phase current when phase A is at the aligned position in the proposed SSRM

When it comes to the nonlinearity of magnetic materials, the saturation effects cannot be ignored. Thus, self and mutual inductances are functions of rotor position and phase currents, and the flux linkage can be written as follows:

$$\psi_k = L_k(i_k, i_{k+1}, \theta)i_k,\qquad(1)$$

where ψ_k represents the flux linkage of phase k, L_k represents the inductance of phase k, i_k represents the phase current of phase k, and i_{k+1} represents the phase current of phase $k+1$.
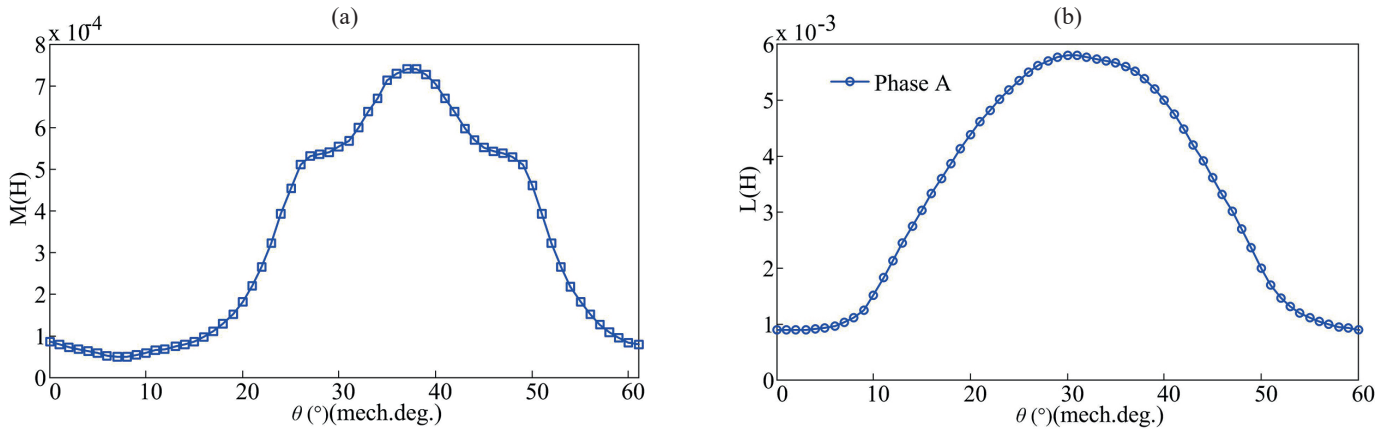
Fig. 4. Mutual inductance and self-inductance of the conventional SRM: a) mutual inductance, b) self-inductance

The inductance can be expressed from the following form [22]:

$$L_k(i_k, i_{k+1}, \theta) = \sum_{n}^{\infty} [f_n(i_k, i_{k+1}, \tau) \cos 2n\theta + \\ + g_n(i_k, i_{k+1}, \tau) \sin 2n\theta], \tag{2}$$

where the functions f_n and g_n depend on the current of phase k and the armature reaction τ.

The flux linkages with only phase A excited and only phase B excited can be respectively drawn as follows:

$$\psi_A = L_A i_A, \tag{3}$$

$$\psi_B = L_B i_B, \tag{4}$$

where L_A and L_B represent the self-inductance of phase A and phase B, respectively, i_A and i_B represent the phase current of phase A and phase B separately.

The flux linkages with both phase A and phase B excited can be drawn in a matrix as follows [23]:

$$\begin{bmatrix} \psi_{AB} \\ \psi_{BA} \end{bmatrix} = \begin{bmatrix} L_A & M_{AB} \\ M_{BA} & L_B \end{bmatrix} \cdot \begin{bmatrix} i_A \\ i_B \end{bmatrix} \tag{5}$$

where ψ_{AB} is the flux linkage of phase A with both phase A and phase B excited, ψ_{BA} is the flux linkage of phase B with both phase A and phase B excited, M_{AB} and M_{BA} are the mutual inductance produced from excitation current i_B to winding A and the mutual inductance produced from excitation current i_A to winding B, respectively.

The total value of the flux linkage can be obtained from (3–5):

$$\psi_{AB} + \psi_{BA} = \psi_A + \psi_B + M_{AB} i_B + M_{BA} i_A \tag{6}$$

The excitation current i_A will be equal to i_B when CCC is adopted, then the mutual inductance could be expressed as follows:

$$M_{AB} = M_{BA} = \frac{\psi_{AB} + \psi_{BA} - \psi_A - \psi_B}{2 i_A} \tag{7}$$

Based on (7), the mutual inductances can be drawn in Figs. 4 and 5. It should be noted that the mutual inductance versus rotor position in the SRM is drawn when the phase current is chosen as 23A, while the mutual inductance versus rotor position in
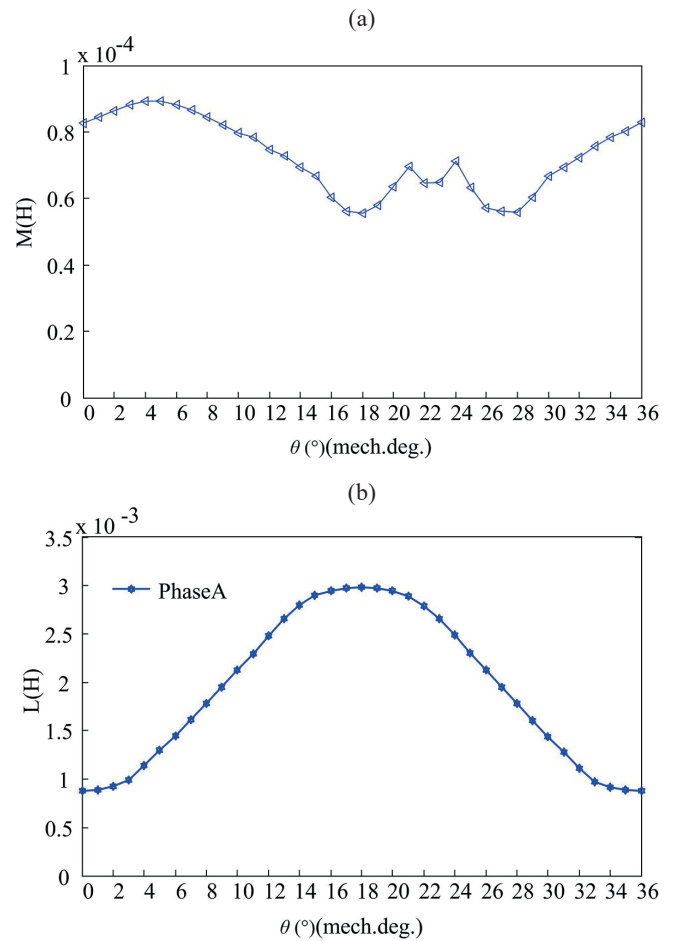

Fig. 5. Mutual inductance and self-inductance of the proposed SSRM: a) mutual inductance, b) self-inductance

the SSRM is drawn when the phase current is chosen as 26A. Self-inductances are also shown in Figs. 4 and 5.

In order to analyze the relationship between mutual inductance and self-inductance quantitatively, the ratio of mean value of mutual inductance and mean value of self-inductance is adopted. All values are listed in Table 2. It can be seen that the ratio of mean value of mutual inductance to mean value of self-inductance M_{AB}/L_A in the proposed SSRM is obviously lesser than that in the conventional SRM, illustrating that the proposed SSRM has less mutual inductance between phases than the conventional SRM.

Table 2
Mean values of mutual inductance and self-inductance

	M_{AB} (mH)	L_A (mH)	M_{AB}/L_A
SRM	0.33	3.2	10.31%
SSRM	0.0726	1.9	3.82%

4. Fault-tolerant operating performance

In this section, the fault-tolerant dynamic performance of the two SRMs is analyzed and compared by FEM under one phase failure condition and half phase failure condition.

The concept of a fault-tolerant motor is that it will continue to operate with the fault and still perform well. The higher fault-tolerant capability a motor possesses, the wider the range of applications for high reliability and safety requirement it will tend to be used in. Consequently, it is of great value to analyze the fault-tolerant operating performance of the motor.

Since winding faults or power converter faults will lead to phase failure, this paper focuses on the fault-tolerant operating performance under one phase failure condition and half phase failure condition due to the space limitation of the research.

4.1. One phase failure. Phase A is selected to simulate one phase failure, the external circuit, mainly composed of an asymmetric half-bridge converter simulated with ANSOFT, is shown in Fig. 6, which is applied to both SRMs, and the simulation
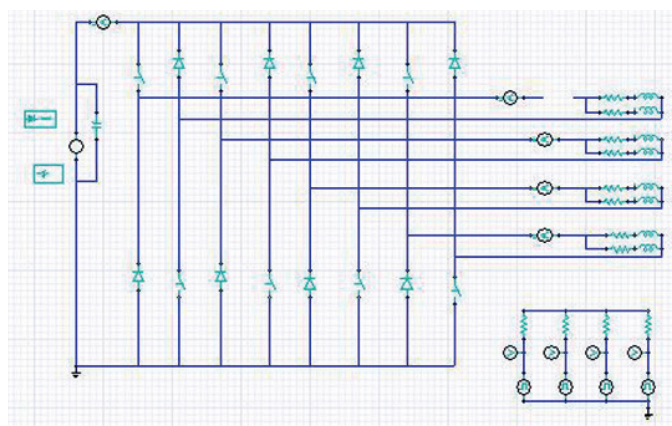
parameters are set as follows: bus voltage U_s is 60 V and the rated speed n_N is 6000 r/min.

4.1.1. Comparison of torque performance. To quantitatively evaluate the torque performance under both healthy and one phase failure operating condition, the average torque and torque ripple are adopted. First, a torque ripple is defined as [24]:

$$K_T = \frac{T_{\max} - T_{\min}}{T_{avg}}, \tag{8}$$

where K_T is the torque ripple coefficient, T_{max}, T_{min}, and T_{avg} are the maximum, minimum, and average values of the output torque, respectively.

Fig. 7 gives the output torque waveforms under both healthy and one phase failure operating conditions in the two SRMs, with more details listed in Table 3. It can be drawn that if one phase failure occurs, the proposed SSRM is still capable of maintaining nearly 80% of its rated torque, while the conventional SRM can only develop about 67% of the rated torque, revealing that the proposed SSRM is able to develop about 13 percentage points more output torque than the conventional SRM. In addition, the torque ripple of the proposed SSRM is

(a)

(b)

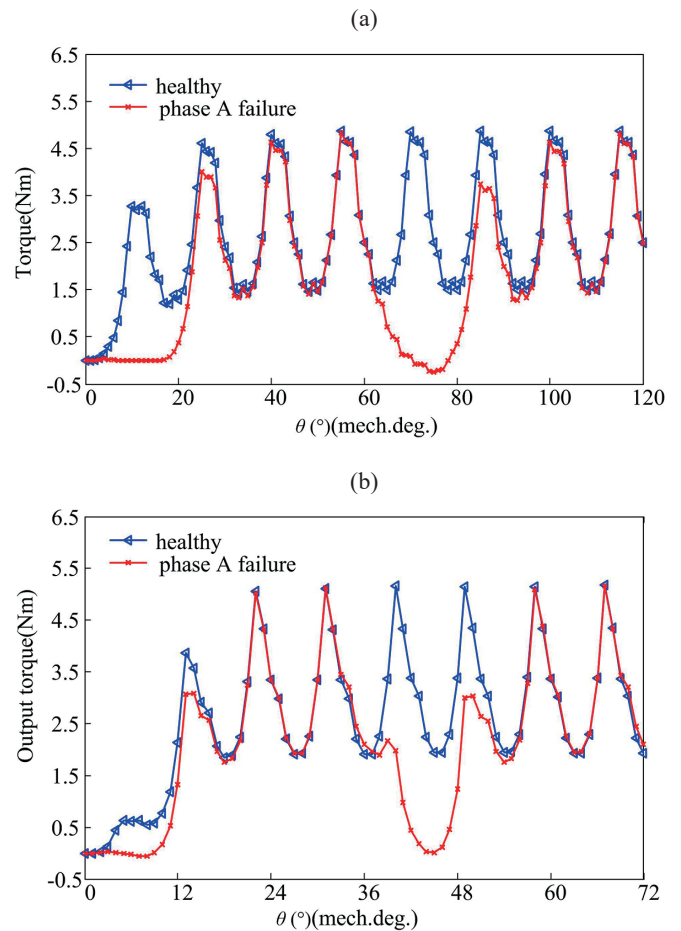Fig. 6. External circuit when phase A is open-circuited

Fig. 7. Output torque values under healthy and one phase failure operating conditions: a) SRM, b) SSRM

smaller than that of the conventional SRM, even though the torque ripples under one phase failure operating condition are relatively larger than those under healthy operating condition. As a result, the comparison of fault-tolerant dynamic performance between these two SRMs clearly emphasizes the superiority of the proposed SSRM.

Table 3
Comparison of the average torque values and torque ripples

Operating condition		SRM	SSRM
Healthy	T_{avg}(Nm)	2.8741	3.1004
	K_T	1.174	1.053
Phase A is open-circuited	T_{avg}(Nm)	1.9067	2.2809
	K_T	2.666	2.257

4.1.2. Comparison of phase currents. Figs. 8 and 9 give the phase current waveforms under both healthy and one phase failure operating conditions in the two SRMs. It can be seen
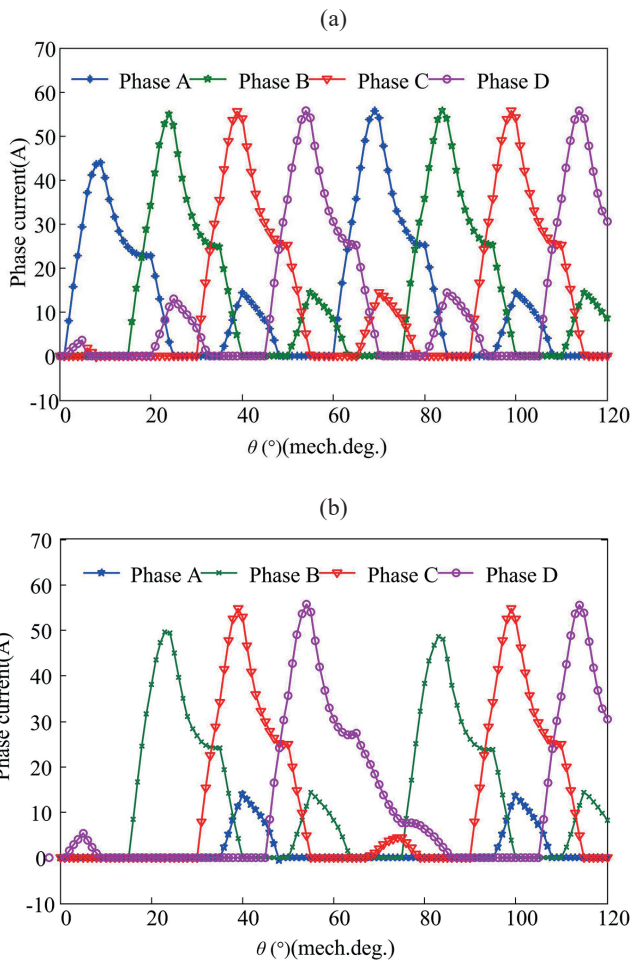
(a)

(b)

Fig. 8. Phase current waveforms of the conventional SRM under healthy and one phase failure operating conditions when phase A is open-circuited: a) healthy, b) one phase failure
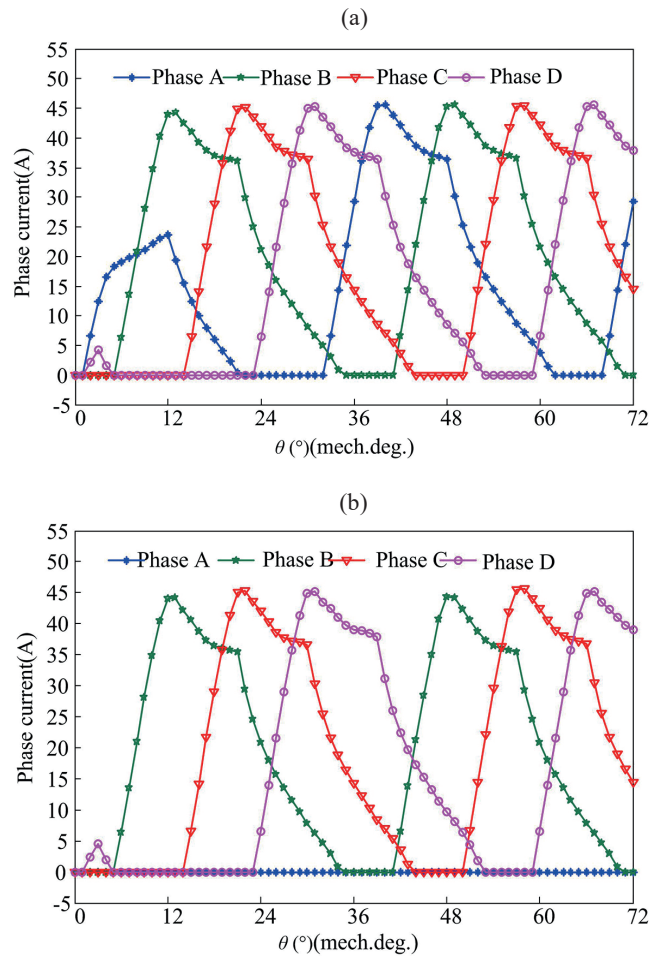
(a)

(b)

Fig. 9. Phase current waveforms of the proposed SSRM under healthy and one phase failure operating conditions: a) healthy, b) one phase failure

from Fig. 8 that the current waveform is inerratic under healthy operating conditions, while the current waveform loses its balance and the induced current of faulty phase A is up to 4A when phase A is open-circuited, which is mainly caused by the symmetry of flux linkage being destroyed, triggering obvious changes in mutual inductance between phases. All these changes just coincide with strong mutual inductance in the conventional SRM, which is verified by Section 3.

In contrast with the conventional SRM, the proposed SSRM shows a distinct difference, which can be seen from Fig. 9. Before and after the phase failure occurs, the current waveforms hardly change, and the induced current of phase A is about zero when phase A fails. These performances result from little mutual inductance between phases in the proposed SSRM, i.e. this motor can keep on operating with one phase failure.

4.2. Half phase failure. In this part, the effect of different winding connection types on the fault-tolerant dynamic performance of the proposed SSRM is discussed. The winding connection in this paper is classified into two types – one is that two coils of one phase are connected in parallel, and the

other is that two coils of one phase are connected in series. The fault-tolerant dynamic performance of the proposed SSRM, in which two coils of one phase are connected in series when half phase fails to work, is the same as that described in Part A. That is because the effect of half phase failing to operate when two coils of one phase are connected in series is equivalent to that of one phase failing. Next, the focus is on fault-tolerant performance when two coils of one phase are connected in parallel.

As can be seen from Fig. 10, both current and torque values of faulty half-phase A are increased, in contrast with those in Fig. 7b and Fig. 9b and torque ripple is smaller than that in Table 3. Consequently, the fault-tolerant dynamic performance of the proposed SSRM where two coils of one phase are connected in parallel is superior to that where two coils of one phase are connected in series, which lays a guiding foundation to the design of fault-tolerant motors.

As the more faulty phases a motor possesses, the more severe fault-tolerant performance it has, a control system or forced shutdown will be adopted rapidly in order to prevent the motors and people from being damaged, which is beyond the scope of this paper.
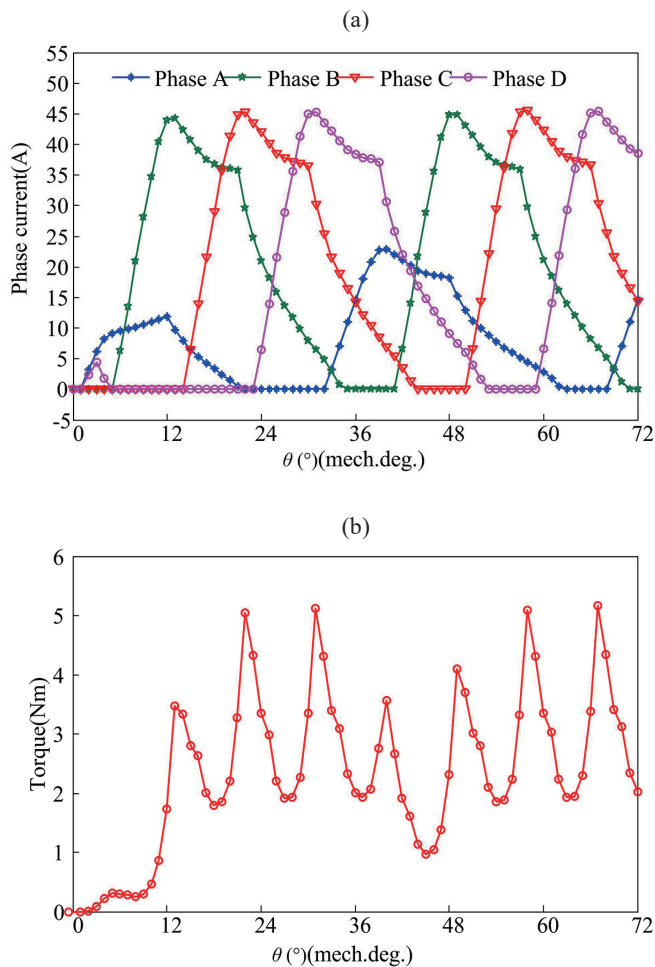

Fig. 10. Phase current and torque waveforms of the proposed SSRM in which two coils of one phase are connected in parallel when half phase fails to work: a) post-fault current, b) Post-fault torque

5. Conclusion

In this paper, comparative analysis on mutual inductance and fault-tolerant dynamic performance under phase failure condition between the proposed SSRM and the conventional SRM is analyzed and examined by 2D FEM. The simulation results reveal that the proposed SSRM has less mutual inductance between phases than the conventional SRM. In addition, if one phase failure occurs, the proposed SSRM is able to develop about 13% more output torque than the conventional SRM, and torque ripple is smaller than that of the conventional SRM. If half phase failure occurs, the fault-tolerant dynamic performance of the proposed SSRM where two coils of one phase are connected in parallel is superior to that where two coils of one phase are connected in series, laying a guiding foundation to the design of the fault-tolerant motors.

REFERENCES

[1] M. Michalczuk, L.M. Grzesiak, and B. Ufnalski, "Hybridization of the lithium energy storage for an urban electric vehicle", *Bull. Pol. Ac.: Tech.* 61 (2), 325–333 (2013).

[2] P. Bogusz, "A switched reluctance motor control method limiting the maximum DC source current in the low-speed range", *Bull. Pol. Ac.: Tech.* 64 (1), 197–206 (2016).

[3] J. Gissing, P. Themann, S. Baltzer, T. Lichius, and L. Eckstein, "Optimal control of series plug-in hybrid electric vehicles considering the cabin heat demand", *IEEE Transactions on Control Systems Technology* 24 (3), 1126–1133 (2016).

[4] L. Szabo and M. Ruba, "Segmental Stator Switched Reluctance Machine for Safety-Critical Applications", *IEEE Transactions on Industrial Applications* 48 (6), 2223–2229 (2012).

[5] S.S.R. Bonthu, J. Baek, M.Z. Islam, and S. Choi, "Optimal design of five phase permanent magnet assisted synchronous reluctance motor for integrated starter generator application", *IEEE International Electric Machines and Drives Conference*, 433–439 (2015).

[6] W. Ding and D. Liang, "A fast analytical model for an integrated switched reluctance starter/generator", *IEEE Transactions on Energy Conversion* 25 (4), 948–956 (2010).

[7] A. Cavagnino, A. Tenconi, and S. Vaschetto, "Experimental characterization of a belt-driven multiphase induction machine for 48 V automotive applications: losses and temperatures assessments", *IEEE Transactions on Industry Applications* 52 (2), 1321–1330 (2016).

[8] X. Sun, L. Chen, Z. Yang, and H. Zhu, "Speed-sensorless vector control of a bearingless induction motor with artificial neural network inverse speed observer", *IEEE/ASME Transactions on Mechatronics* 18 (4), 1357–1366 (2013).

[9] X. Sun, L. Chen, H. Jiang, Z. Yang, J. Chen, and W. Zhang, "High-performance control for a bearingless permanent magnet synchronous motor using neural network inverse scheme plus internal model controllers", *IEEE Transactions on Industrial Electronics* 63 (6), 3479–3488 (2016).

[10] X. Sun, L. Chen, and Z. Yang, "Overview of bearingless permanent magnet synchronous motors", *IEEE Transactions on Industrial Electronics* 60 (12), 5528–5538 (2013).

[11] X. Sun, Z. Shi, L. Chen, and Z. Yang, "Internal model control for a bearingless permanent magnet synchronous motor based on inverse system method", *IEEE Transactions on Energy Conversion* 31 (4), 1539–1548 (2016).

[12] Y. Guo, J. Zhu, H. Lu, Z. Lin, and Y. Li, "Core loss calculation for soft magnetic composite electrical machines", *IEEE Transactions on Magnetics* 48 (1), 3112–3115 (2012).

[13] Y. Guo, J. Zhu, H. Lu, Y. Li, and J. Jin, "Core loss computation in a permanent magnet transverse flux motor with rotating fluxes", *IEEE Transactions on Magnetics* 50 (11), Art. Seq. No. 6301004 (2014).

[14] G. Lei, Y.G. Guo, J.G. Zhu, T.S. Wang, X.M. Chen, and K.R. Shao, "System level six sigma robust optimisation of a drive system with PM transverse flux machine", *IEEE Transactions on Magnetics* 48 (2), 923–926 (2012).

[15] G. Lei, C.C. Liu, J. Zhu, and Y. Guo, "Robust multidisciplinary design optimization of PM machines with soft magnetic composite cores for batch production", *IEEE Transactions on Magnetics* 52 (3), Art. Seq. No. 8101304 (2016).

[16] A.G. Jack, B.C. Mecrow, and J.A. Haylock, "A comparative study of permanent magnet and switched reluctance motors for high-performance fault-tolerant applications", *IEEE Transactions on Industry Applications* 38 (4), 889–895 (1996).

[17] T. Roubache, S. Chaouch, and M.S.N. Said, "Sensorless fault-tolerant control of an induction motor based electric vehicle", *Journal of Electrical Engineering and Technology* 11 (5), 1423–1432 (2016).

[18] G.H. Liu, M. Chen, and W.X. Zhao, "Design and analysis of five-phase fault-tolerant interior permanent-magnet Vernier machine", *IEEE Transactions on Applied Superconductivity* 26 (4), Art. Seq. No. 0604805 (2016).

[19] H. Shin, K.B. Lee, "Optimal design of a 1 kW switched reluctance generator for wind power systems using a genetic algorithm", *IET Electric Power Applications* 10 (8), 807–817 (2016).

[20] Q. Chen, G.H. Liu, W.X. Zhao, M.M, Shao, and Z.M. Liu, "Design and analysis of the new high-reliability motors with hybrid permanent magnet material", *IEEE Transactions on Magnetics* 50 (12), Art. Seq. No. 8207010 (2014).

[21] B.N. Qu, and J.C. Song, T. Liang, H.D. Zhang, "Mutual coupling and its effect on torque waveform of even number phase switched reluctance motor", *International Conference on Electrical Machines and Systems*, 3405–3410 (2008).

[22] F. Piriou, A. Razek, "Calculation of saturated inductances for numerical simulation of synchronous machine", *IEEE Transactions on Magnetics* 19 (6), 2628–2631, (1983).

[23] J.Ye, B. Bilgin, and A. Emadi, "Elimination of mutual flux effect on rotor position estimation of switched reluctance motor drives", *IEEE Transactions on Power Electronics* 30 (3), 1499–1512 (2015).

[24] J. Ye, B. Bilgin, and A. Emadi, "An extended-speed low-ripple torque control of switched reluctance motor drives", *IEEE Transactions on Power Electronics* 30 (3), 1457–1470 (2015).